



Mechanical behavior of TiN/CrN nano-multilayer thin film deposited by unbalanced magnetron sputter process

Pei-Ling Sun^a, Cherng-Yuh Su^b, Tai-Pin Liou^b, Cheng-Hsun Hsu^c, Chung-Kwei Lin^{a,*}

^a Department of Materials Science and Engineering, Feng Chia University, Taichung 407, Taiwan

^b Department of Mechanical Engineering, National Taipei University of Technology, Taipei 106, Taiwan

^c Department of Materials Engineering, Tatung University, Taipei 104, Taiwan

ARTICLE INFO

Article history:

Received 22 August 2010

Received in revised form 2 December 2010

Accepted 8 December 2010

Available online 15 December 2010

Keywords:

Unbalanced magnetron sputtering

TiN

CrN

Nanoindentation

Thermal stability

ABSTRACT

TiN and CrN single layer thin films along with TiN/CrN multilayer thin film, which has an average layer thickness of 4 nm were deposited on WC substrates by a commercially used unbalanced DC magnetron sputtering. The microstructure and mechanical properties of the as-deposited films were investigated. The TiN/CrN multilayer thin film has a single phase structure with the preferential orientation of (2 0 0), a finer surface morphology and a finer columnar crystal structure. Additionally, the TiN/CrN multilayer thin film also shows better adhesion on substrate and hardness than the single layer thin films. The hardness of the annealed multilayer thin film is slightly increased after annealed at temperatures of 600–800 °C. This is attributed to the increased intensity of (1 1 1) reflection during annealing.

© 2010 Elsevier B.V. All rights reserved.

1. Introduction

Protective coating deposition has been employed on the metal tool surface to increase the tool life [1,2]. Solid ceramic thin films made of transition metal nitrides or carbides, such as TiN, TiCN, TiAlN and CrN, have been extensively used as hard coating thin films. However, tools with a single layer nitride or carbide coatings are still not sufficiently hard enough for practical application. On the other hand, higher hardness coatings, such as TiC or diamond-like carbon thin films, have low toughness. Additionally, the temperature raise during tool use may cause thin film oxidation; for instance, rapid oxidation of TiN film can occur at 600 °C [3]. This oxidation phenomenon leads to coating degradation and failure. Films without high-temperature thermal stability may not meet the functional requirement.

Thin films with alternating depositions of two (or more) materials have recently attracted considerable attention because of the material mechanical properties can be significantly improved. Multilayer thin films generally exhibit enhanced mechanical properties and thermal stability compared to their single layer counterparts [4–7]. For example, a study of Chang et al. showed that nano-scaled TiAlN/CrN multilayered coatings with a bi-layer thickness ranging from 6 to 12 nm have high hardness values of ~36 GPa [6]. Mul-

tilayered TiN/SiN_x coatings exhibited enhanced thermal stability compared to the single layer counterpart [7]. Chen et al. showed that the multilayered structure can be preserved after annealing at 1000 °C when the SiN_x layer thickness is ~0.8 nm of multilayered TiN/SiN_x coatings [5]. It was concluded that the smaller the bi-layer period thickness is, the better these properties are before a critical value is reached [6,7].

In this work, a commercial unbalanced magnetron (UBM) sputter deposition system was used to deposit TiN and CrN single layer thin films on tungsten carbide substrates with various parameters. TiN/CrN multilayer thin films were deposited with the optimal processing parameters obtained from deposition of TiN and CrN single layer thin films. The mechanical properties, including hardness and attrition resistance, and the thermal stability of the single layer and multilayer coatings, were investigated.

2. Experimental procedures

A commercial UBM sputter system was utilized to deposit TiN and CrN single layer thin films and TiN/CrN multilayer thin films on tungsten carbide substrates. This UBM system is equipped with a DC power supply (Advanced Energy, Pinnacle Plus+) with a maximum power of 10 kW. A flat-type target with a dimension 520 mm × 80 mm × 8 mm was used for deposition. An applied bias voltage ranging from 0 to –300 V was used. Substrate was rotated along its main axis to orient it in the proper position for deposition. Single layer and multilayer thin films were then deposited on the substrate.

Single layer TiN and CrN films were deposited with the controlled nitrogen flow rates of 20, 25 and 30 sccm. The optimal processing parameters were then selected to deposit TiN/CrN multilayer thin films by controlling the individual layer thickness. The film morphology and microstructure were observed in a LEO 1530 field emission

* Corresponding author. Tel.: +886 4 24517250x5309; fax: +886 4 24510014.

E-mail address: cklin@fcu.edu.tw (C.-K. Lin).

scanning electron microscope (FESEM). Cross-sectional microstructures of the thin films were then examined in order to measure the thickness and the deposition rate can be calculated. The crystal structures of the thin films were characterized by X-ray diffraction (XRD). The XRD measurements at Cu K α wavelength of 1.541 Å were performed on MAC Science M03-XHF XRD with a scan speed of 3°/min at the 2 θ angles of 30–90°.

The mechanical properties and thermal stability of the multilayer thin films were also investigated. Hardness test (MTS, Nano Indenter XP) and scratch test (CSEM, Scratch Tester) were included to evaluate the mechanical properties. Nanoindentation tests were performed with a Berkovich indenter under a maximum load of 50 mN. Scratch adhesion testing was carried out with a diamond indenter that has a radius of 200 μ m scratching on the thin films with the load of 0–100 N, constant loading rate of 100 N/min and scratch speed of 10 mm/min. The critical load (L_c) was defined as the normal load that film starts to spall or separate from the substrate, which was monitored by acoustic emission (A. E.) and confirmed by optical microscope. Thermal stability was examined using a rapid thermal annealing (RTA) system (ULVAC, QHC-P610C Rapid Thermal Annealing). The samples were heated at 20 °C/min to 400, 600, 800 and 1000 °C after deposition and maintained at that fixed temperature for 1 h. The mechanical properties of the annealed TiN/CrN multilayer thin films were measured and compared with the as-deposited thin film to evaluate the thermal stability.

3. Results and discussion

The film morphology, crystal structure and the mechanical property of the as-deposited thin films were investigated. The XRD patterns of selected TiN and CrN single layer thin films (deposited with nitrogen flow rate of 30 sccm) along with the TiN/CrN multilayer thin film are shown in Fig. 1. The major reflections that can be clearly observed in TiN and CrN single layer films are (1 1 1), (2 0 0) and (2 2 0) planes. The preferential orientation of TiN phase is (1 1 1) whereas it is (2 0 0) in CrN phase. The TiN/CrN multilayer thin film XRD pattern exhibits a single phase structure, in which the (1 1 1) reflection is the average of the (1 1 1) positions of TiN and CrN phases. Additionally, the spectrum shows superlattice reflections on both sides of the main (1 1 1) reflection. This indicates the presence of multilayer structure. Similar to the TiN and CrN single layer thin films, TiN/CrN multilayer thin film exhibits (1 1 1), (2 0 0) and (2 2 0) reflections but with the preferential orientation of (2 0 0).

The surface morphology and cross-sectional microstructure of the TiN/CrN multilayer thin films were observed in FESEM and the secondary electron images (SEI) are shown in Fig. 2. Compared to the TiN and CrN single layer thin films [8], the TiN/CrN multilayer thin film displays a finer surface morphology and columnar crystal structure. The total thickness of the thin film was derived from the cross-sectional image (Fig. 2a) and it is 1.77 μ m. Therefore, the

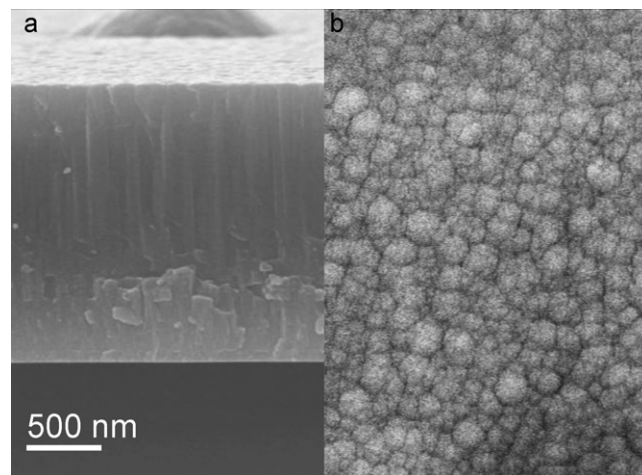


Fig. 2. Secondary electron images of cross section and top view of the as-deposited TiN/CrN multilayer thin film.

average layer thickness can be calculated from the total thickness dividing by substrate rotation numbers and gives a number of 4 nm.

The mechanical properties of the samples were evaluated by nanoindentation scratch test and hardness test. Fig. 3 shows the A. E. signal as a function of indenter loading of the TiN single layer, CrN single layer and TiN/CrN multilayer thin films. The curve shows that critical load (L_c) is not at where the A. E. signal launched. This is caused by some small fractures on the two sides of scratch before thin film failure happened and therefore interfered the A. E. signals. It can be seen that the critical loads are 24.7 N, 34.5 N and 45.1 N for TiN single layer, CrN single layer and TiN/CrN multilayer thin films, respectively. Critical loads were also investigated as a function of the nitrogen flow rate in the single layer thin films (see Fig. 4). The number indicates the nitrogen flow rate. The average critical load was calculated from two tests. Critical load is not influenced by the nitrogen flow rate in TiN single layer thin films whereas the intermediate nitrogen flow rate can contribute to higher critical load in CrN thin films. TiN/CrN multilayer thin film has the highest critical load (45.1 N) which means that the adhesion on the substrate is significantly improved in the multilayer thin film compared to the single layer thin films.

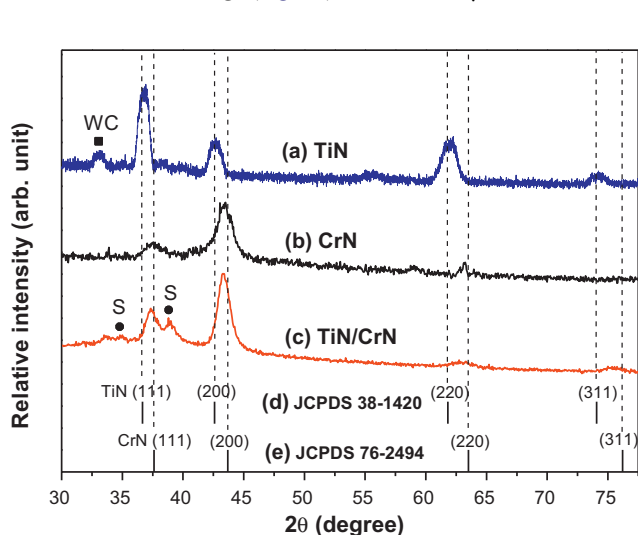


Fig. 1. XRD patterns of (a) TiN single layer thin film, (b) CrN single layer thin film, (c) TiN/CrN multilayer thin film, (d) TiN JCPDS 38-1420 and (e) CrN JCPDS 76-2494. S indicates superlattice reflections.

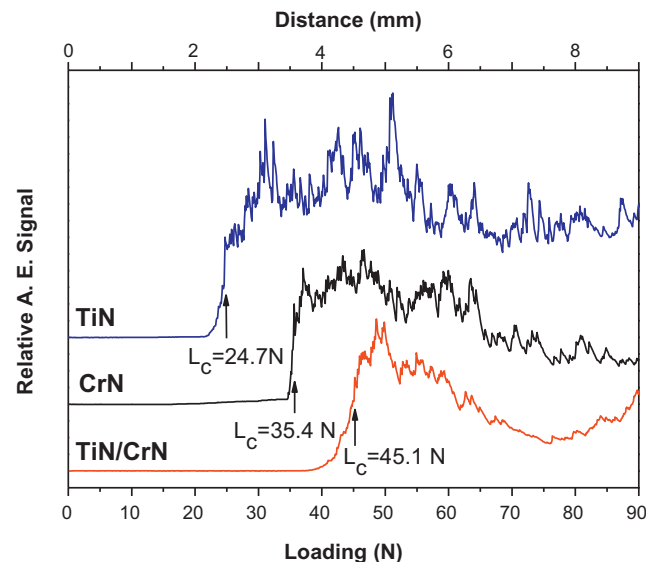


Fig. 3. Scratch test results of TiN single layer, CrN single layer and TiN/CrN multilayer thin films.

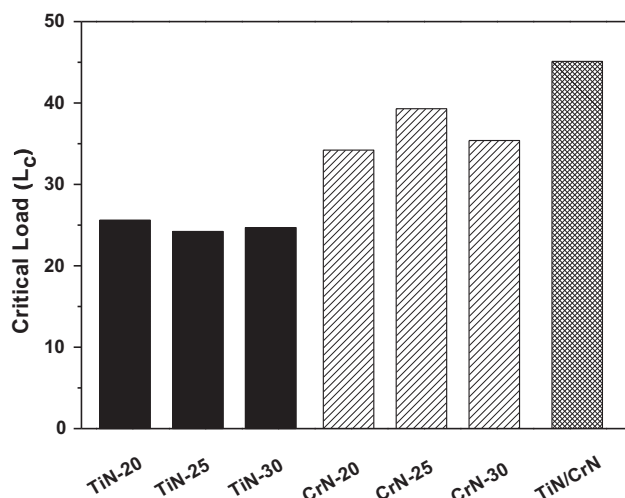


Fig. 4. Critical loads of TiN and CrN single layers processed by different nitrogen flow rates and TiN/CrN multilayer thin film.

In general, hardness tests of thin films only investigate the small indentation depth. In this work, a large indentation depth (~ 1100 nm) was applied to reflect the substrate effect. The hardness of different nitrogen flow rates was recorded as a function of indentation depth in TiN and CrN single layer thin films (Fig. 5a and b). It is seen that the hardness increases with indentation depth to ~ 200 nm and followed by a drop in all single layer thin films. The hardness remains unchanged after 300 nm in the TiN single layer thin films but it shows a continuous but slight decline in the CrN single layer thin films. The increase of hardness at small indentation depth is attributed to the transition between purely elastic to elastic/plastic deformation. Nitrogen flow rate does not notably affect the hardness value.

The variation of hardness with indentation depth of the selected TiN and CrN single layer thin films (deposited with nitrogen flow rate of 30 sccm) and TiN/CrN multilayer thin film are shown in Fig. 6. The maximum hardness values are similar in the two single layer thin films (23.9 ± 0.4 GPa in TiN and 21.4 ± 0.9 GPa in CrN). Similar to the single layer thin films, the hardness of TiN/CrN multilayer thin film increases with indentation depth to ~ 200 nm but followed by slight hardening to indentation depth of 1100 nm. The hardness of the TiN/CrN multilayer thin film (34.8 ± 0.2 GPa) is much higher compared to the single layer thin films. High strength of multilayer thin film is partially caused by the fine grain structure, which is typically of the order of the thin film thickness and partially by dislocation-related activities, in which the critical stress needed to move a dislocation depends on the thin film thickness [9] and many interfaces can block dislocation movement [10]. The hardness decrease at indentation depth larger than ~ 200 nm was also observed in TiN/TaN multilayer thin films [11], and it was attributed to the Si substrate effect. It is expected that substrate effect becomes more important with increasing indentation depth. Additionally, the indentation size effect (ISE) also plays an important role [12]. It was experimentally proved that the hardness decreases with increasing indentation depth based on the presence of strain gradients in the deformation zone around the indent [12]. However, the hardening behavior in the TiN/CrN multilayer thin film reveals that the substrate effect and ISE become negligible in the multilayer thin films.

Thermal stability of the TiN/CrN multilayer thin film was also investigated. Fig. 7 shows the XRD patterns of the as-deposited and annealed TiN/CrN multilayer thin films. It can be seen that the multilayer thin film is thermally stable up to 800°C . No oxide was formed until 1000°C was reached. The hardness tests were car-

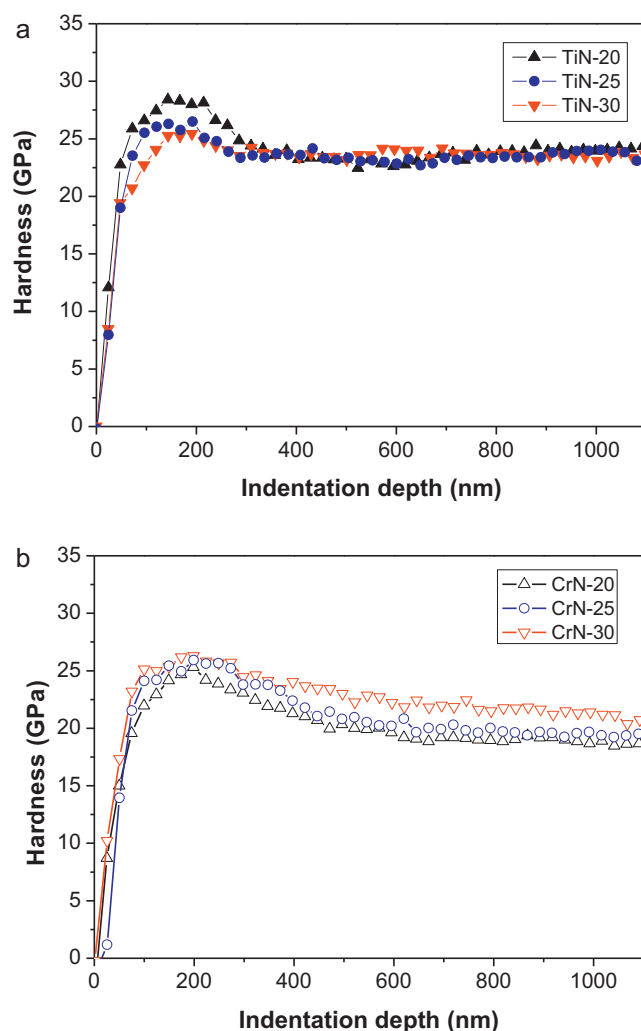


Fig. 5. Hardness versus indentation depth in (a) TiN single layer and (b) CrN single layer thin films processed by different nitrogen flow rates.

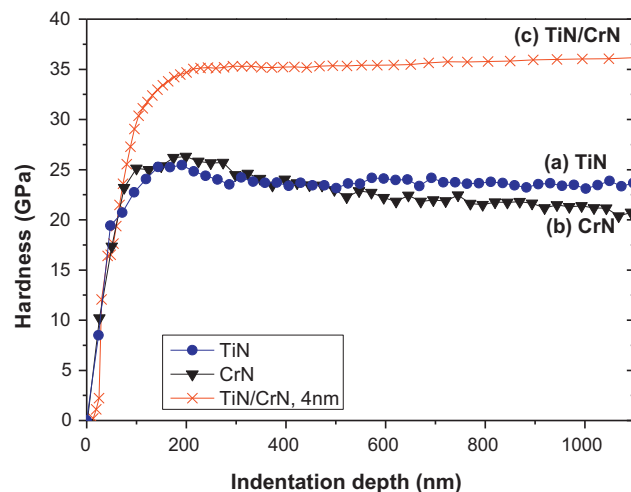


Fig. 6. Hardness versus indentation depth in TiN single layer, CrN single layer and TiN/CrN multilayer thin films.

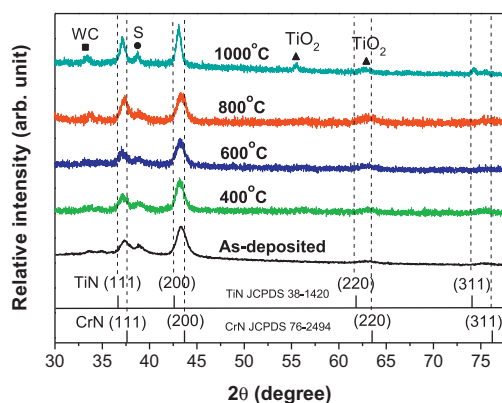


Fig. 7. XRD patterns of the as-deposited and annealed TiN/CrN multilayer thin films. S indicates superlattice reflections.

ried out on the as-deposited and annealed samples. Fig. 8 shows the hardness variation as a function of indentation depth of the as-deposited and annealed TiN/CrN multilayer thin films. It is seen that all the hardness of the four curves increase with indentation depth to ~200 nm. The as-deposited thin film shows a continuous hardening to 1100 nm. The annealed thin films show similar trend except there is a drop after 200 nm. Similar observation was found in Al/Cu thin films [9] and it was attributed to the surface roughness effect. It is not clear why the hardness drops after 200 nm indentation depth in this work. Yield drop phenomenon was recently observed in ultrafine-grained pure aluminum [13,14]. An explanation of yield drop in LiF crystal was proposed by Johnston and Gilman [15], which is caused by the shortage of mobile dislocations in the specimen to fulfill the applied strain rate. In a crystal with fairly low mobile dislocations, the moving dislocations start with a high velocity and therefore a high stress is needed. When the dislocations start to move, dislocations multiply rapidly, and contribute to a lower velocity. The low velocity gives to low stress and therefore yield drop occurs. It is therefore speculated that dislocation activity related work has caused a significant influence on the hardness drop in this work. More work of dislocation analysis is suggested in order to clarify this issue.

It is interesting that the hardness increases slightly with increasing annealing temperature in the present work except at 400 °C. Lower hardness value at 400 °C annealed thin film is attributed to partial strain relief. Compared to other work in the literature,

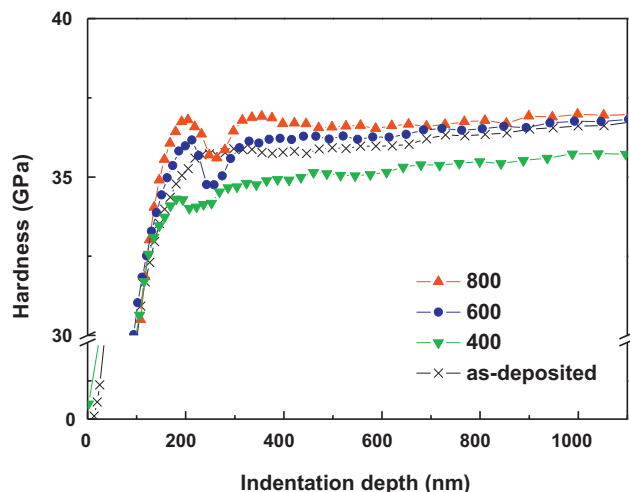


Fig. 8. Nanoindentation results of TiN/CrN multilayer thin films after annealed at different temperatures.

Barshilia et al. [16] showed that the hardness of TiN/CrN multilayer thin film decreases with increasing annealing temperature. The decrease is a result of inter-diffusion at the interfaces, which usually occurs in the multilayer structure when it is annealed. On the other hand, the work of Kim et al. [17] showed that the hardness in TiN/AlN multilayer is maintained up to 1000 °C because the coherent lattice between TiN and AlN layers can still be maintained. Chen et al. [5] showed that the hardness in TiN/SiN multilayer thin film increased when the thin films were annealed at 1000 °C because the TiN crystallinity can be improved. In this work, the (200) preferential orientation of the TiN/CrN multilayer thin film becomes weaker therefore the contribution of (111) reflection becomes more important with increasing annealing temperature (Fig. 7). It is suggested that (111) texture in TiN layer is more efficient to block dislocation movement and facilitate to higher hardness [18]. The same observation was found in a TiAlN/CrN multilayer thin film [6]. It shows that with the increase of (111) intensity ratio, the hardness value increases because of the (111) preferred orientation growth has the highest atomic packing density [6]. This is also proved in this work, in which slight increase in hardness with annealing temperature results from the increase of (111) reflection intensity.

The present study proved that the TiN/CrN multilayer thin films have enhanced thermal stability and mechanical properties. The adhesion on the substrate is significantly improved in the multilayer thin film compared to the single layer thin films. The hardness of the multilayer thin film is also enhanced and can be even slightly increased after annealing at the temperatures of 600–800 °C with the absence of oxide. This indicates that the TiN/CrN multilayer thin film deposited by the UBM sputtering system exhibited good thermal stability up to 800 °C as well as improved mechanical properties.

4. Conclusion

TiN single layer, CrN single layer and a TiN/CrN multilayer thin film were deposited on WC substrates by using a commercial unbalanced magnetron sputtering system. The morphology, crystal structure, and mechanical properties of the as-deposited thin films were evaluated. The TiN/CrN multilayer thin film has an average layer thickness of 4 nm and exhibits a single phase structure with the preferential orientation of (200). The surface morphology and columnar crystal structure are finer in the TiN/CrN multilayer thin film compared to the TiN and CrN single layer thin films.

TiN/CrN multilayer thin film also shows better adhesion on substrate and hardness than the single layer thin films. The hardness of the annealed multilayer thin film is slightly increased after annealing at the temperatures of 600–800 °C. This is attributed to the increase intensity of (111) reflection after annealing. This work indicates that the TiN/CrN multilayer thin film deposited by the UBM sputtering system exhibited good thermal stability up to 800 °C as well as improved mechanical properties.

Acknowledgement

This work was supported by the National Science Council of Taiwan under contract no. NSC 95-2622-E-027-030-CC3.

References

- [1] W.D. Sproul, Surf. Coat. Technol. 81 (1996) 1–7.
- [2] V. Derflinger, H. Brändle, H. Zimmermann, Surf. Coat. Technol. 113 (1999) 286–292.
- [3] L.A. Donohue, I.J. Smith, W.D. Münz, I. Petrov, J.E. Greene, Surf. Coat. Technol. 94–95 (1997) 226–231.
- [4] I. Wadsworth, I.J. Smith, L.A. Donohue, W.D. Münz, Surf. Coat. Technol. 94–95 (1997) 315–321.

- [5] Y.H. Chen, M. Guruz, Y.P. Chung, L.M. Keer, *Surf. Coat. Technol.* 154 (2002) 162–166.
- [6] C.L. Chang, J.Y. Jao, W.Y. Ho, D.Y. Wang, *Vacuum* 81 (2007) 604–609.
- [7] T. An, M. Wen, L.L. Wang, C.Q. Hu, H.W. Tian, W.T. Zheng, *J. Alloys Compd.* 486 (2009) 515–520.
- [8] C.Y. Su, C.T. Pan, T.P. Liou, P.T. Chen, C.K. Lin, *Surf. Coat. Technol.* 203 (2008) 657–660.
- [9] W.D. Nix, *Mater. Sci. Eng. A234–236* (1997) 37–44.
- [10] X. Chu, S.A. Barnett, *J. Appl. Phys.* 77 (1995) 4403–4411.
- [11] J. An, Q.Y. Zhang, *Surf. Coat. Technol.* 200 (2005) 2451–2458.
- [12] W.J. Poole, M.F. Ashby, N.A. Fleck, *Scripta Mater.* 34 (1996) 559–564.
- [13] N. Tsuji, Y. Ito, Y. Minamino, Y. Saito, in: T.G. Langdon, et al. (Eds.), *Ultrafine Grained Materials II*, TMS, 2002.
- [14] C.Y. Yu, P.W. Kao, C.P. Chang, *Acta Mater.* 53 (2005) 4019–4028.
- [15] W.G. Johnston, J.J. Gilman, *J. Appl. Phys.* 30 (1959) 129–144.
- [16] H.C. Barshilia, A. Jain, K.S. Rajam, *Vacuum* 72 (2004) 241–248.
- [17] D.G. Kim, T.Y. Seong, Y.J. Baik, *Surf. Coat. Technol.* 153 (2002) 79–83.
- [18] M.A. Auger, O. Sanchez, C. Ballesteros, M. Jergel, M. Aguilar-Frutis, C. Falcony, *Thin Solid Films* 433 (2003) 211–216.